Inorganic Chemistry
Article

Inorg. Chem. **2010**, *49*, 5845–5852 **5845**
DOI: 10.1021/ic9025816

Formation Mechanism of TiO_2-Derived Titanate Nanotubes Prepared by the Hydrothermal Process

Atsushi Nakahira,*,†,‡ Takashi Kubo,*,† and Chiya Numako*,§

†*Department of Materials Science, Graduate School of Engineering, Osaka Prefecture University, 1-1 Gakuencho, Naka-ku, Sakai, Osaka 599-8531, Japan,* ‡*Institute of Materials Research, Osaka Center, Tohoku University, 1-1 Gakuencho, Naka-ku, Sakai, Osaka 599-8531, Japan, and* §*Department of Natural System, Faculty of Integrated Science, University of Tokushima, 2-24 Shinzocho, Tokushima 770-8502, Japan*

Received December 28, 2009

The structural change on the molecular scale of anatase-type TiO_2 during hydrothermal treatment was investigated in detail by various analytic techniques such as X-ray absorption fine structure and transmission electron microscopy in order to clarify the formation mechanisms of titanate-based nanotubes. It revealed that the nanosheet-like products composed of highly distorted TiO_6 octahedra were generated by hydrothermal treatment of anatase-type TiO_2, and then the anatase-like structures are partially built up with the formative nanotubes by scrolling up these nanosheet-like products and nanosheets.

1. Introduction

Nanomaterials with one-dimensional nanostructures have attracted much attention because of their potential applications in a variety of novel devices.[1] Especially, TiO_2-derived nanotubes,[2] which are prepared by hydrothermal treatment of TiO_2 particles in a concentrated NaOH aqueous solution, are expected to be useful for several application studies such as electrochromism,[3] bone regeneration,[4] proton conduction,[5] photoinduced hydrophilicity,[6] photocatalysts,[7−10] and dye-sensitizing solar batteries.[11] Recently, many attempts on the morphologic control such as preparations of film and bulk for these nanotubes have been carried out extensively in order to make full use of the characteristics of TiO_2-derived nanotubes as several applications.[3,6,12−16] It is also desirable to control the size and morphology in order to improve their functional properties. For example, ribbonlike potassium and sodium titanate has been successfully synthesized by improving an alkali solution synthetic process.[17−19] However, the crystalline structure and formation mechanism of TiO_2-derived nanotubes are still topics under discussion. The elucidation of the crystalline structure and formation mechanism for TiO_2-derived nanotubes will be expected to lead to the further development of novel functional materials with one-dimensional nanostructures.

It has been discussed whether obtained TiO_2-derived nanotubes are anatase-type TiO_2 or a titanate compound. Tsai et al. and Yang et al. have reported that the final pH value of the washing water after the washing process had much effect on the structure of the nanotubes, and the layered titanate transformed into a nanotube through $Na^+ \rightarrow H^+$ substitution on the washing process and eventually transformed into anatase-type TiO_2.[20−22] In their previous study, the

*To whom correspondence should be addressed. E-mail: nakahira@mtr.osakafu-u.ac.jp (A.N.), kubo-t@mtr.osakafu-u.ac.jp (T.K.), numako@ias.tokushima-u.ac.jp (C.N.).

(1) Iijima, S. *Nature* **1991**, *354*, 56.
(2) Kasuga, T.; Hirashima, M.; Hoson, A.; Sekino, T.; Niihara, K. *Langmuir* **1998**, *14*, 3160.
(3) Tokudome, H.; Miyauchi, M. *Angew. Chem., Int. Ed.* **2005**, *44*, 1974.
(4) Kubota, S.; Johkura, K.; Asanuma, K.; Okouchi, Y.; Ogiwara, N.; Sasaki, K.; Kasuga, T. *J. Mater. Sci.: Mater. Med.* **2004**, *15*, 1031.
(5) Thorne, A.; Kruth, A.; Tunstall, D.; Irvine, J. T. S.; Zhou., W. *J. Phys. Chem. B* **2005**, *109*, 5439.
(6) Tokudome, H.; Miyauchi, M. *Chem. Commun.* **2004**, 958.
(7) Adachi, M.; Murata, Y.; Harada, M.; Yoshikawa, S. *Chem. Lett.* **2000**, *29*, 942.
(8) Akita, T.; Okumura, M.; Tanaka, K.; Ohkuma, K.; Kohyama, M.; Koyanagi, T.; Date, M.; Tsubota, S.; Haruta, M. *Surf. Interface Anal.* **2005**, *37*, 265.
(9) Nakahira, A.; Kubo, T.; Yamasaki, Y.; Suzuki, T.; Ikuhara, Y. *Jpn. J. Appl. Phys.* **2005**, *44*, 690.
(10) Kubo, T.; Nagata, H.; Takeuchi, M.; Matsuoka, M.; Anpo, M.; Nakahira, A. *Res. Chem. Intermed.* **2008**, *34*, 339.
(11) Uchida, S.; Chiba, R.; Tomiha, M.; Masaki, N.; Shirai, M. *Electrochemistry* **2002**, *70*, 418.
(12) Tian, Z. R.; Voigt, J. A.; Lin, J.; Mckenzie, B.; Xu, H. *J. Am. Chem. Soc.* **2003**, *125*, 12384.
(13) Liu, A.; Wei, M.; Honma, I.; Zhou, H. *Anal. Chem.* **2005**, *77*, 8068.
(14) Kubo, T.; Yamasaki, Y.; Nakahira, A. *J. Mater. Res.* **2007**, *22*, 1286.
(15) Yada, M.; Inoue, Y.; Uota, M.; Torikai, T.; Watari, T.; Noda, I.; Hotokebuchi, T. *Lamgmuir* **2007**, *23*, 2815.
(16) Yada, M.; Inoue, Y.; Uota, M.; Torikai, T.; Watari, T.; Noda, I.; Hotokebuchi, T. *Chem. Mater.* **2008**, *20*, 346.
(17) Lim, S. H.; Luo, J.; Zhong, Z.; Ji, W.; Lin, J. *Inorg. Chem.* **2005**, *44*, 4124.
(18) Wang, C.; Deng, Z. X.; Li, Y. *Inorg. Chem.* **2001**, *40*, 5210.
(19) Sun, X.; Chen, X.; Li, Y. *Inorg. Chem.* **2002**, *41*, 4996.
(20) Yang, J.; Jin, Z.; Wang, X.; Li, W.; Zhang, J.; Zhang, S.; Guo, X.; Zhang, Z. *Dalton Trans.* **2003**, 3898.
(21) Tsai, C. C.; Teng, H. *Chem. Mater.* **2004**, *16*, 4352.

Published on Web 06/08/2010

nanotubes prepared by washing treatments at pH values of 5−13 were composed of a titanate compound, and the nanotubes prepared by acidic post-treatment washing at pH values of 0−2 had X-ray diffraction (XRD) patterns analogous to that of anatase-type TiO_2 rather than that of the titanate compound. In terms of the formation mechanism, it has been generally recognized that the nanotubes are formed by scrolling sheets exfoiled from titanate compounds such as $A_2Ti_3O_7$,[23−31] $A_2Ti_2O_4(OH)_2/A_2Ti_2O_5 \cdot H_2O$,[20−22,32] or lepidocrocite-type $A_xTi_{2-x/4}\square_{x/4}O_4$ (A = Na and/or H; □ = vacancy).[33−35] On the other hand, Kukovecz et al. pointed out some major shortcomings of the currently accepted sheet rollup mechanism and proposed the oriented nanotube crystal growth from nanoloop seeds as a mechanism.[36] Tsai et al. and Yang et al. reported the mechanism for nanotube formations.[37,38] Thus, the investigation of the formation mechanism of TiO_2-derived nanotubes is now of specific interest and important.

Our previous study revealed that TiO_2-derived nanotubes prepared by the hydrothermal process (the final pH value of the washing water was 6.8−7 for the HCl washing process) were mainly composed of layered titanate and the anatase-like structure was partly present in the titanate-based nanotubes.[39−42] This formation of the anatase-like structure was thought to be caused by consolidation of the nanotubes. In the present work, the structural change on the molecular scale of anatase-type TiO_2 involved in the formative nanotube was investigated in detail by various analytical methods such as X-ray absorption fine structure (XAFS) and transmission electron microscopy (TEM) in order to clarify the detailed formation mechanism of TiO_2-derived titanate-based nanotubes.

2. Experimental Section

A total of 2 g of anatase-type TiO_2 powder (3 m^2/g; Kojundo Chemicals, Saitama, Japan) with a particle size of ca. 50 nm or a metal titanium plate (10 mm × 10 mm × 0.1 mm, Niraco, Japan) as the starting material was used. Specimens were added in a 10 M NaOH aqueous solution (20 mL). Then the specimens were treated under hydrothermal reaction at 383 K for 1−96 h. Obtained products after hydrothermal treatments were sufficiently washed with deionized water and a dilute HCl aqueous solution (0.1 M) and were subsequently separated from the washing solution by filtration. This treatment was repeated until the washing water showed pH < 7. The final pH value of the washing water was 6.8−7. After washing treatment, they were filtered and subsequently dried at temperatures above 323 K for more than 12 h in an electric oven.

Phase identification was carried out by a XRD method (Rint 2100, Rigaku Co., Ltd., Tokyo, Japan) using Cu Kα radiation at 40 kV and 20 mA. The XRD profiles were collected between 2θ angles of 5 and 60° with a step interval of 0.02° and scanning rate of 1°/min. Various microstructural analyses were performed by a field-emission scanning electron microscopy (FE-SEM; S-4500, Hitachi, Tokyo, Japan) with and accelerating voltage of 15 kV and by TEM (JEM2010/SP, JEOL, Tokyo, Japan) with an accelerating voltage of 200 kV. Nitrogen adsorption isotherms at 77 K were obtained by an automatic gas adsorption measurement apparatus (BELSORP 18PLUS-SPL, BEL Japan, Osaka, Japan). Some pieces of product were pretreated at 403 K for 10 h.

Ti K-edge X-ray absorption near-edge structure (XANES) and extended X-ray absorption fine structure (EXAFS) were recorded at room temperature with BL01B1 in a SPring 8 with the Japan Synchrotron Radiation Research Institute (a ring energy of 8 GeV and a stored current of about 100 mA). The Ti K-edge XAFS data for this study were collected by transmission mode using a Si(111) double-crystal monochromator ($2d$ = 0.627 nm). The data were collected using ionization chambers filled with gas (I_0 chamber, $He/N_2 = 7/3$; I chamber, N_2). For XAFS measurements, the samples were prepared as pellets with the thickness varied to obtain a 0.5−1 jumps at the Ti K-edge absorption. Ti metallic foil was used to carry out for the energy calibration. XANES was analyzed by subtracting a linear background computed by a least-squares fitting from the pre-edge region and normalized segment. EXAFS spectra were analyzed by using standard methods. The pre-edge region was subtracted, and then the EXAFS spectrum was extracted by fitting the absorption coefficient with a cubic spline method. In most cases, k^3 weighting was used in the analysis and Fourier transforms were taken between k = 2.5 and 12 $Å^{-1}$. The Fourier transformation of the k^3-weighted EXAFS oscillation from k space to r space was performed over the range 2.5−12 $Å^{-1}$ to obtain a radial distribution function (FT-EXAFS). Analysis of the EXAFS data was conducted using the commercial software *REX2000* (Rigaku Co., Ltd., Tokyo, Japan).

3. Results and Discussion

Figure 1 shows typical SEM images of products prepared by hydrothermal treatments of anatase-type TiO_2 at 383 K for 1−96 h. From the results of SEM observations, the morphology of the product prepared by hydrothermal treatment for 1 h did not change (Figure 1b). However, it was clearly shown that the morphology of anatase particles started to change and the nanotube-like products were observed on the surface of TiO_2 after hydrothermal treatment for 3 h (Figure 1c). With an increase of the time of hydrothermal treatments, a lot of nanotube-like products were synthesized for 6 h (Figure 1d) and for 12 h (Figure 1e). After 96 h of hydrothermal treatment, large amounts of nanotube products were synthesized. These observations of the microstructure change of the product with the

(22) Tsai, C. C.; Teng, H. *Chem. Mater.* **2006**, *18*, 367.
(23) Du, G. H.; Chen, Q.; Che, R. C.; Yuan, Y.; Peng, L. M. *Appl. Phys. Lett.* **2001**, *79*, 3702.
(24) Chen, Q.; Du, G. H.; Zhang, S.; Peng, L. M. *Acta Crystallogr., Sect. B* **2002**, *58*, 2002.
(25) Chen, Q.; Zhou, W.; Du, G. H.; Peng, L. M. *Adv. Mater.* **2002**, *14*, 1208.
(26) Zhang, S.; Peng, L. M.; Chen, Q.; Du, G. H.; Dawson, G.; Zhou, W. Z. *Phys. Rev. Lett.* **2003**, *91*, 256103.
(27) Sun, X.; Li, Y. *Chem.—Eur. J.* **2003**, *9*, 2229.
(28) Yuan, Z. Y.; Su, B. L. *Colloids Surf. A* **2004**, *241*, 173.
(29) Bavykin, D. V.; Parmon, V. N.; Lapkin, A. A.; Walsh, F. C. *J. Mater. Chem.* **2004**, *14*, 3370.
(30) Zhang, S.; Chen, Q.; Peng, L. M. *Phys. Rev. B* **2005**, *71*, 014104.
(31) Bavykin, D. V.; Frendrich, J. M.; Alexei, A.; Lapkin, A. A.; Walsh, F. C. *Chem. Mater.* **2006**, *18*, 1124.
(32) Nian, J. N.; Teng, H. S. *J. Phys. Chem. B* **2006**, *110*, 4193.
(33) Ma, R.; Bando, Y.; Sasaki, T. *Chem. Phys. Lett.* **2003**, *380*, 577.
(34) Ma, R.; Sasaki, T.; Bando, Y. *J. Am. Chem. Soc.* **2004**, *126*, 10382.
(35) Ma, R.; Fukuda, K.; Sasaki, T.; Osada, M.; Bando, Y. *J. Phys. Chem. B* **2005**, *109*, 6210.
(36) Kukovecz, A.; Hodos, M.; Horvath, E.; Radnoczi, G.; Konya, Z.; Kiricsi, I. *J. Phys. Chem. B* **2005**, *109*, 17781.
(37) Tsai, C. C.; Teng, H. *Chem. Mater.* **2004**, *16*, 4352.
(38) Yang, J.; Jin, Z.; Wang, X.; Li, W.; Zhang, J.; Zhang, S.; Guo, X.; Zhang, Z. *Dalton Trans.* **2003**, 3898.
(39) Nakahira, A.; Kato, W.; Tamai, M.; Isshiki, T.; Nishio, K.; Aritani, H. *J. Mater. Sci.* **2004**, *39*, 4239.
(40) Kubo, T.; Kato, W.; Yamasaki, Y.; Nakahira, A. *Key Eng. Mater.* **2006**, *317&318*, 247.
(41) Kubo, T.; Yamasaki, Y.; Nakahira, A. *J. Ion Exchange* **2007**, *18*, 310.
(42) Kubo, T.; Nakahira, A. *J. Phys. Chem. C* **2008**, *112*, 1658.

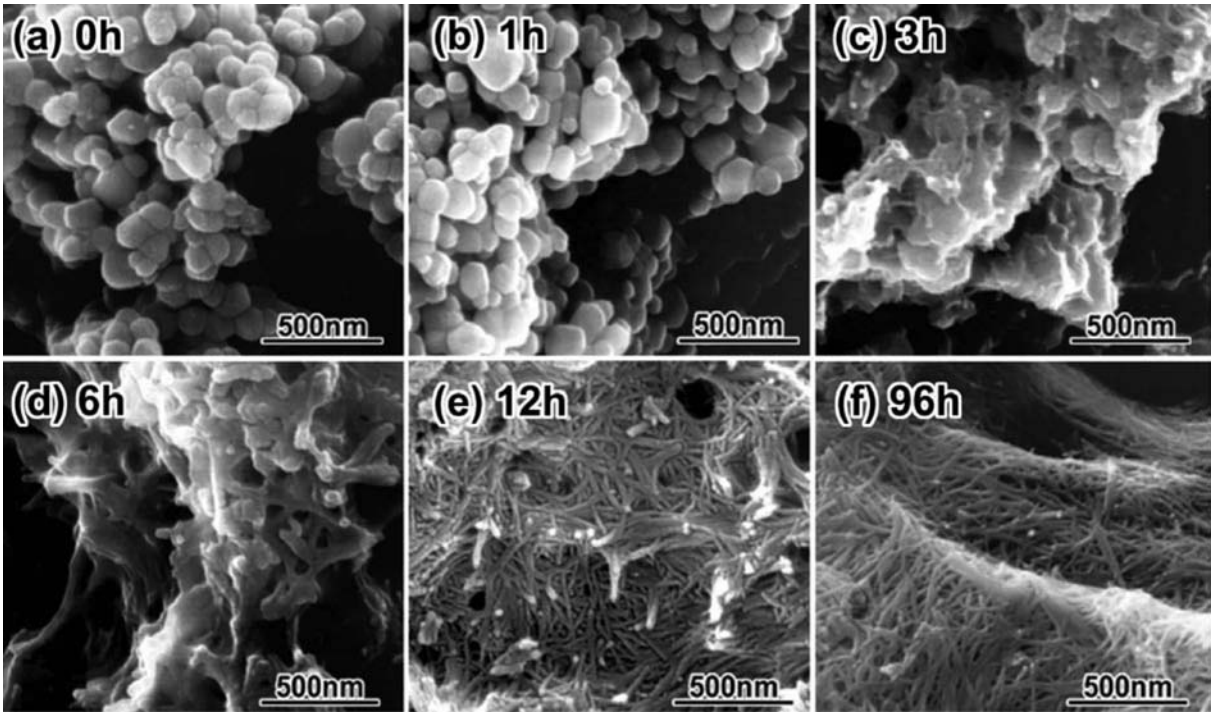

Figure 1. SEM images of the products prepared by hydrothermal treatments of anatase-type TiO_2 at 383 K for (a) 0 h (anatase), (b) 1 h, (c) 3 h, (d) 6 h, (e) 12 h, and (f) 96 h.

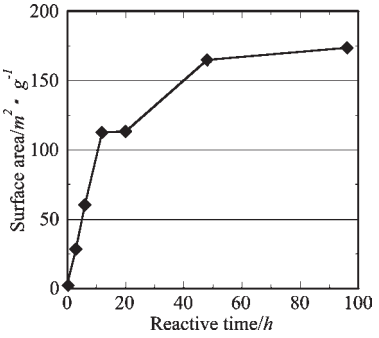

Figure 2. BET surface area values obtained by nitrogen adsorption measurement for hydrothermally treated products.

hydrothermal time suggested that the nanotube-like products were first generated on the surface of TiO_2 powder as a starting material in the stage of the initial term of the hydrothermal reaction. Furthermore, the effect of the sodium content on the microstructure of nanotubes is important. Therefore, energy-dispersive X-ray (EDX) evaluation was carried out for products prepared by hydrothermal treatment for 3−96 h. The Na/Ti atomic ratio for products prepared by hydrothermal treatment for 96 h was approximately 0.2 without acid treatment with a 0.1 M HCl aqueous solution. On the contrary, after acid treatment with a 0.1 M HCl aqueous solution, sodium could not be detected in this sample by EDX analysis, and consequently sodium could be removed from the products. Therefore, the influence of the sodium content is negligible for the products in this study.

Figure 2 shows the Brunauer−Emmett−Teller (BET) surface area values estimated by nitrogen adsorption measurement for hydrothermally treated products. Furthermore, from nitrogen adsorption measurement, it was found that the BET value dramatically increased according to this

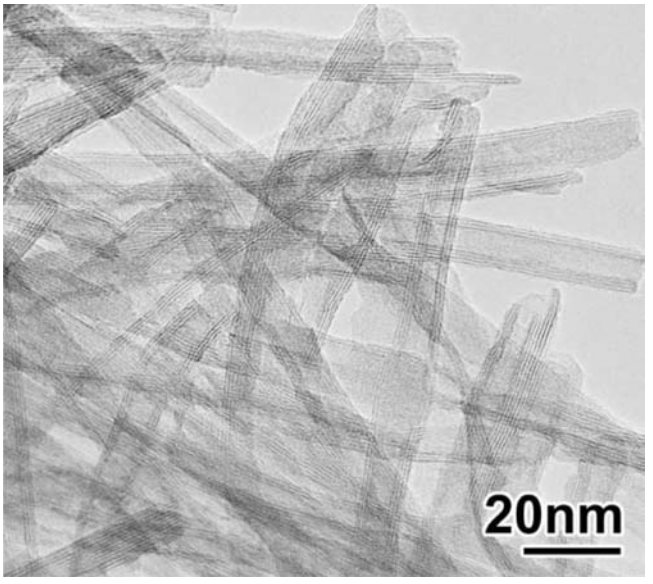

Figure 3. Typical TEM image of the product prepared by hydrothermal treatment of anatase-type TiO_2 at 383 K for 96 h.

change of morphology. The SEM images and BET surface area values of each sample indicated that nanotubes were formed in hydrothermal treatment for 3−6 h. The morphology of anatase particles has been completely changed into a nanowhisker after hydrothermal treatment for 96 h (Figure 1f). According to TEM observation, it was obvious that these nanowhisker-shaped products were nanotubes with about 10 nm outer diameter, 5 nm inner diameter, and a few hundred nanometers length (Figure 3). Figure 4 shows the XRD results of the products prepared by hydrothermal treatments of anatase-type TiO_2 at 383 K for 0, 3, 6, 12, 48, and 96 h. XRD profiles showed that a synthesized product

prepared by hydrothermal treatment for 96 h had a single phase for anatase-type TiO_2, although unreacted anatase existed in the products after hydrothermal treatments for 1−48 h (Figure 4). The products synthesized by hydrothermal treatments for 6, 12, and 48 h were composed of a mixture of anatase (for 0 h reaction) and nanotubes (for 96 h reaction). This nanotubular product prepared by hydrothermal treatment for 96 h had a high BET surface area value of approximately 200 m^2/g. FT-IR measurements were done for anatase and the dried nanotubular product, as was previously reported.[40] For the nanotubular products, three absorption bands centered at 3400, 1630, and 950 cm^{-1} are assigned to the O−H stretching mode for interlayer water, oxonium ions, and hydroxyl groups, H−O−H bending for water and oxonium ions, and O−H bending for hydroxyls, respectively. These results indicate the most replacement of Na^+ in the nanotubular product by H^+.

Typical TEM images of products prepared by hydrothermal treatments of anatase-type TiO_2 for 3 and 6 h and anatase-type TiO_2 as the starting material are shown in Figure 5. Nanosheet-like products, as shown in Figure 5b, were observed on the surface of an anatase-type TiO_2 particle after hydrothermal treatment for 3 h by TEM. The selected-area electron diffraction (SAED) of these nanosheet-like products nearly showed a halo pattern, implying that these nanosheet-like products were identified as not crystalline TiO_2 but amorphous. In the case of hydrothermal treatment for 6 h, nanotubular products with scrolled structures were observed in large numbers (Figure 5c). The synthesis of TiO_2-derived nanotubes was also attempted through the same treatment as that for a metal titanium plate,[40] and products on the metal titanium plate were observed by TEM. Figure 6 shows that scrolling of nanosheet-like products on the surface of a titanium plate was observed by TEM for the hydrothermally treated titanium plate in a 10 M NaOH aqueous solution at 383 K for 3 h. These products prepared by hydrothermal treatment of a titanium plate were the same nanotubes as those from anatase TiO_2. Because the surface of a titanium metal has thin films of titanium oxide, we carried out hydrothermal treatment under the same conditions as those for titanium as well as anatase in order to understand the mechanism of nanotube formation. As shown in Figure 6, scrolling of nanosheet-like products, i.e., layered sodium titanate, was still observed on the titanium plate by TEM observations. These observations suggest that, in the primary stage of hydrothermal treatment, the nanosheet-like products

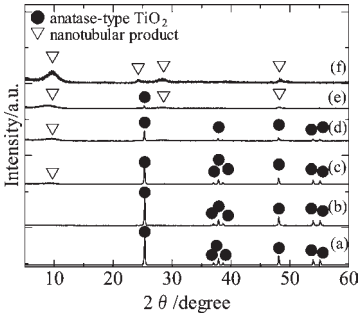

Figure 4. XRD patterns of the products prepared by hydrothermal treatments of anatase-type TiO_2 at 383 K for (a) 0 h (anatase), (b) 3 h, (c) 6 h, (d) 12 h, (e) 48 h, and (f) 96 h.

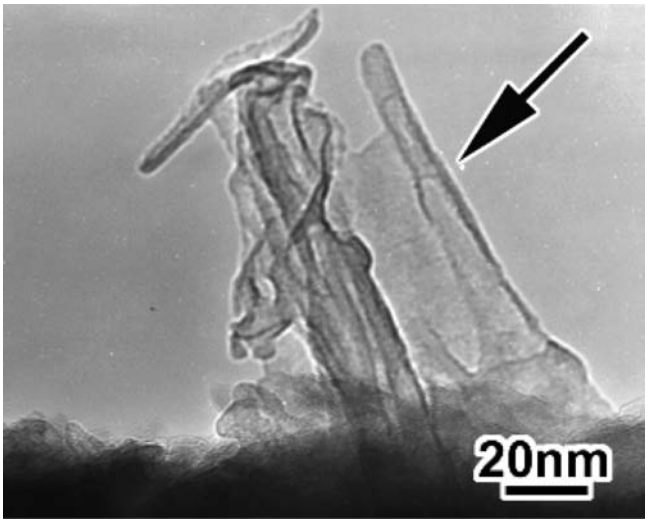

Figure 6. TEM image of a titanium plate hydrothermally treated in a 10 M NaOH aqueous solution at 383 K for 3 h.

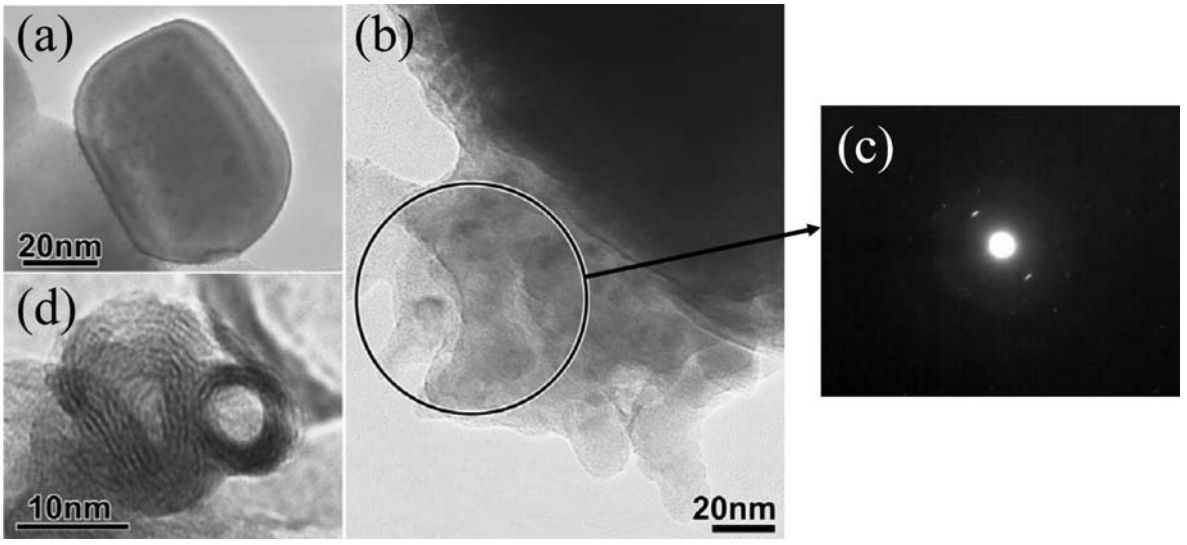

Figure 5. TEM images of products prepared by hydrothermal treatments of anatase-type TiO_2 at 383 K for (a) 0 h (anatase), (b) 3 h, and (d) 6 h. (c) SAED pattern of the area enclosed by the circle in part b.

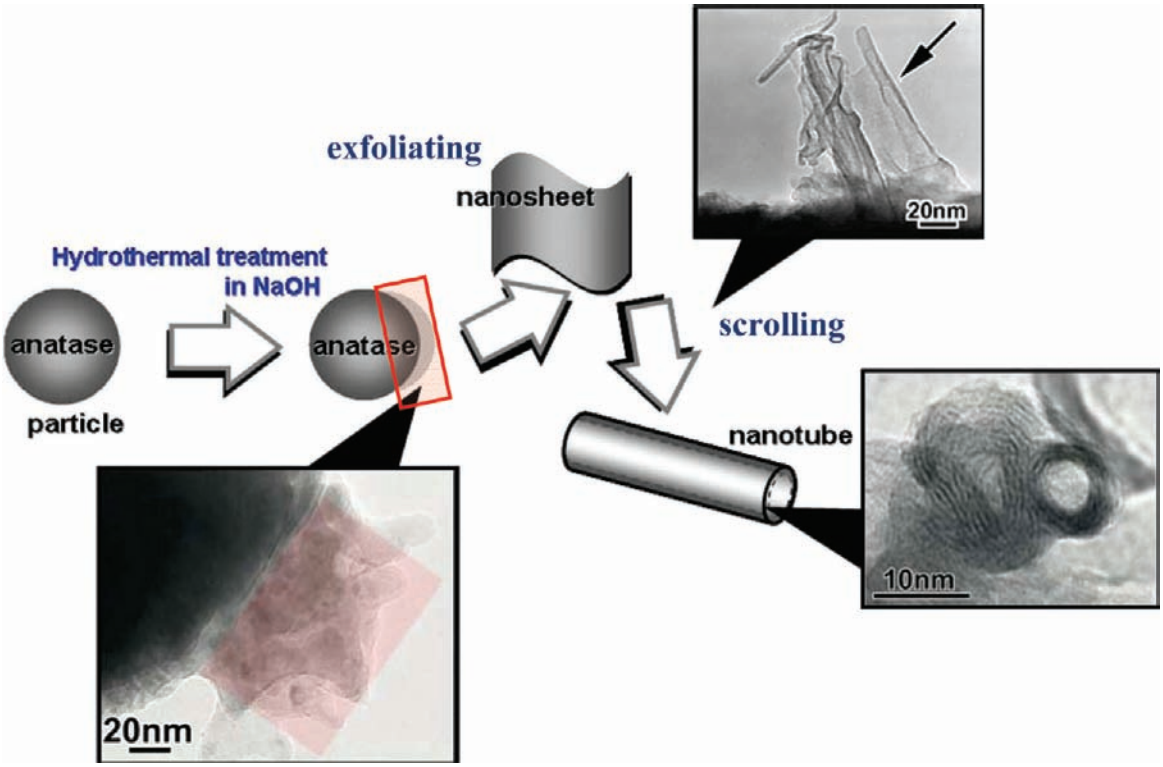

Figure 7. Schematic drawing of the exfoliation and scrolling mechanism of nanosheets for nanotubular products in these experiments.

(layered sodium titanate) were preferentially formed and, subsequently, their nanosheets were exfoliated from layered sodium titanate and then the nanosheets were curled and scrolled to nanotubes.

The nanosheets grow with the increasing tendency of curling, leading to the formation of nanotubes by exfoliation of layer sheets from layered sodium titanate. The surface tension caused by the charge of the surface of layer sheets of layered sodium titanate during excessive intercalation of Na^+ between layered sodium titanate on the primary stage of hydrothermal treatments is closely related with exfoliation and scrolling of nanosheets, leading to the formation of nanotubes. Discussion about the driving force for nanotube formation from a nanosheet is underway, although various mechanisms are proposed. In this study, the nanotube formation from anatase TiO_2 is proposed in Figure 7. Figure 7 shows the schematic drawing of the exfoliation and scrolling mechanism of nanosheets for nanotubular products in these experiments. As shown in Figure 7, we proposed the following the three-stage mechanism for nanotube formation:

(1) Nanosheet-like products, i.e., layer sheets of layered sodium titanate from layered sodium titanate, are formed on the surface of TiO_2 during the primary stage of hydrothermal treatments.
(2) Subsequently, nanosheets are exfoliated.
(3) Curling and scrolling of exfoiliated nanosheets lead to nanotube formation.

Consequently, it is concluded that the scrolling mechanism of an exfoliated TiO_2-derived nanosheet is dominant for nanotube formation

The structural changes of anatase-type TiO_2 with the formation of nanotubes in a hydrothermal process were investigated from information on the local structure around titanium by Ti K-edge XAFS (EXAFS and XANES) measurements. Figure 8 shows k^3-weighted EXAFS ocsillations for products prepared by hydrothermal treatments at 383 K for 0 h (anatase), 3 h, 6 h, and 96 h. Figure 9 shows the Fourier-transformed (FT) EXAFS for anatase-type TiO_2 and products prepared by hydrothermal treatments for 3, 6, and 96 h. These represent a radial distribution function plot around the Ti atoms. Furthermore, in order to obtain the structural parameters, the curve fitting of the nearest Ti−O shell was performed by inverse FT. The structural values were obtained from simulation of the experimental spectrum using the theoretical curves calculated by Mckale et al.[42,43] The inverse FT of the first-shell single and the best fit for each sample are shown in Figure 8. In all samples, the agreement between the two curves is quite satisfactory. The parameters obtained by EXAFS analysis are summarized in Table 1. As shown in Figures 8 and 9, the magnitude of the first peak and the smaller subsequent ones at higher r in FT-EXAFS with an increase in the reaction time, implying a lowering of the crystallinity or generation of some vacancies of the neighboring atoms such as O. Furthermore, the nearest Ti−O peak for anatase-type TiO_2 broadened and shifted toward smaller distances through hydrothermal treatment. The shift of the nearest Ti−O peak toward smaller distances and the difference of the peak geometry are thought to be due to highly distorted TiO_6 octahedra. Thus, the results of EXAFS analysis indicate that the geometry of TiO_6 octahedra in anatase-type TiO_2 changed with consolidation of the nanotubes.

Figure 10A shows background-subtracted and normalized Ti K-edge XANES spectra for hydrothermally treated samples, anatase-type TiO_2, rutile-type TiO_2, Ti_2O_3, and TiO. The edge region in the absorption spectra provides much

(43) Mckale, A. G.; Veal, B. W.; Paulikas, A. P.; Chan, S. K.; Knapp, G. S. *J. Am. Chem. Soc.* **1988**, *110*, 3763.

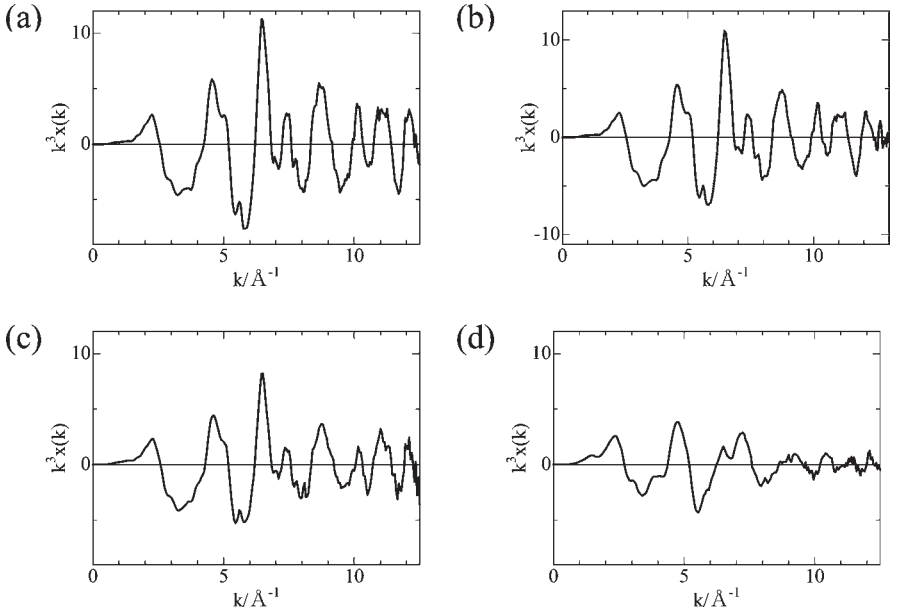

Figure 8. k^3-weighted EXAFS oscillations for products prepared by hydrothermal treatments at 383 K for 0 h (anatase), 3 h, 6 h, and 96 h.

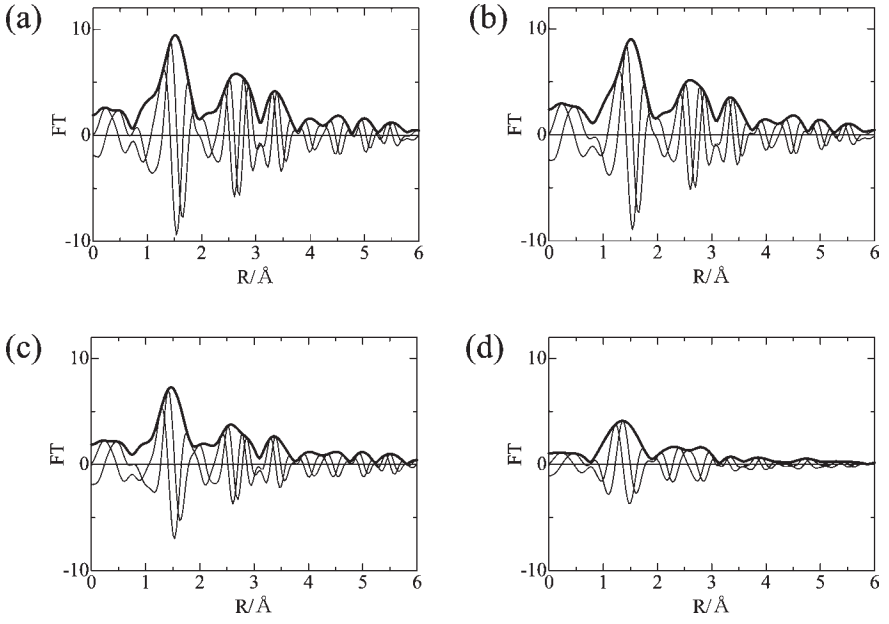

Figure 9. FT-EXAFS for products prepared by hydrothermal treatments of anatase-type TiO_2 at 383 K for (a) 0 h (anatase), (b) 3 h, (c) 6 h, and (d) 96 h.

Table 1. Nearest Ti−O Distance and Average Coordination Number for Products Prepared by Hydrothermal Treatments at 383 K for 0 h (Anatase), 3 h, 6 h, and 96 h

reaction time/h	nearest Ti−O distance	average coordination number
0	1.96	6
3	1.95	5.7
6	1.95	5.5
96	1.92	5.2

information on the environment geometry and the electronic structure of the absorption atom. Figure 10B shows the first derivative regions of Ti K-edge XANES spectra shown in Figure 10A. The edge energy is defined as the energy position corresponding to the peak maximum of the first derivative function. Through hydrothermal treatment, XANES spectra revealed a lower-energy position for the peak maximum of the first derivative function (edge energy), although the peak positions of the hydrothermally treated products were very close to the peak position of TiO_2. It is considered that the shift of the edge energy might be caused by the presence of some oxygen vacancies. As shown in Figure 10A, the characteristic pre-edge peaks were also observed at 4960−4970 eV. The pre-edge peak can be assigned to forbidden transitions from the core 1s level to unoccupied 3d states of Ti ^{IV}.

The pre-edge peaks of Ti K-edge XANES for anatase TiO_2, hydrothermally treated samples, and layered $K_2Ti_2O_5$ as a reference sample are shown in Figure 11. $K_2Ti_2O_5$ as a reference can be selected as a layered titanate material containing five-coordinate titanium.[42] The pre-edge spectrum of anatase TiO_2 contains three major features in this region (peaks A, C, and D in Figure 11). According to the previous studies, the origin of peak A is assigned to an exciton

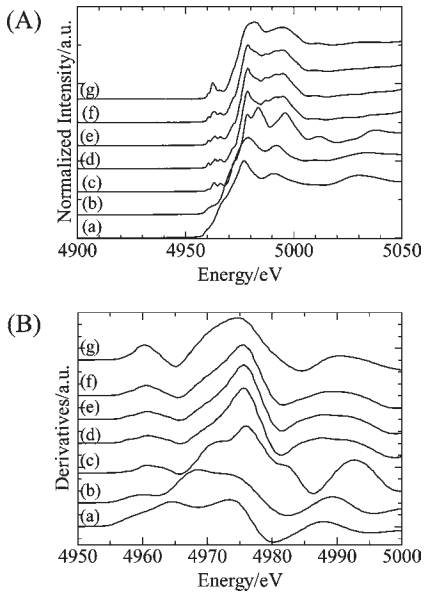

Figure 10. (A) Ti K-edge XANES for (a) TiO, (b) Ti_2O_3, (c) rutile, and products prepared by hydrothermal treatments for (d) 0 h (anatase), (e) 3 h, (f) 6 h, and (g) 96 h. (B) First-derivative functions of Ti K-edge XANES spectra shown in part A.

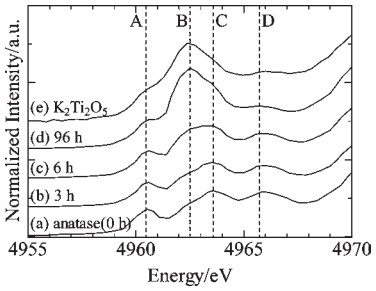

Figure 11. Pre-edge spectra of Ti K-edge XANES for products prepared by hydrothermal treatments of anatase-type TiO_2 at 383 K for (a) 0 h (anatase), (b) 3 h, (c) 6 h, (d) 96 h and (e) $K_2Ti_2O_5$.

band or a transition from $1s \rightarrow 1t_{1g}$.[42−48] The peaks C and D are attributed to the $1s \rightarrow 3d$ transition and designated as $1s \rightarrow 2t_{2g}$ and $1s \rightarrow 3e_g$ transitions (e_g = electronic transitions), respectively.[42−45] Furthermore, Chen et al. reported that peak C reflects the distortion from the octahedral TiO_6 unit and the intensity at peak C increases with the distortion from the octahedral TiO_6 unit. Other studies also suggested that a substantial distortion of the octahedral titanium site results in an increase of the relative intensity for peak C.[45] As shown in Figure 11, the intensity of peak C for products prepared by hydrothermal treatments for 3 and 6 h increased, compared with anatase TiO_2 as the starting material. With progression of the hydrothermal reaction, the structure of the octahedral TiO_6 unit from anatase unsurprisingly changed and, as a consequence, the intensity of peak C positively increased. Accordingly, the increase of distortion from the octahedral TiO_6 unit during hydrothermal treatments implies the progression of the hydrothermal reaction, being consistent with the results of XRD and TEM. Therefore, the change of the intensity at peak C in Figure 11 suggests that anatase TiO_2 as the starting material reacted with products of nanosheet/nanotube during hydrothermal treatment.

On the contrary, in the pre-edge spectrum of $K_2Ti_2O_5$ with five-coordinate titanium, a strong peak was located at 4961 eV. This peak B is thought to be assigned to the allowed $1s \rightarrow t_{2g}$ transition for tetrahedral symmetry, suggesting that such a peak dominates the pre-edge XANES of layered sodium titanate ($K_2Ti_2O_5$) containing five-coordinate titanium.[42] As shown in the figure, the peak was located at 4961 eV (peak B) in the pre-edge spectrum of Ti K-edge XANES for a sample prepared by hydrothermal treatment for 6 h, indicating that the five-coordinate titanium species are locally present in this sample. Therefore, the nanosheet-like product and nanosheets in the products prepared by hydrothermal treatments for 3 and 6 h might have five-coordinate titanium, implying that these nanosheet-like products and nanosheets were composed of the highly distorted TiO_6 octahedra. Furthermore, progression of the hydrothermal reaction (the increase of the hydrothermal reaction time) led to an increase of the intensity of peak B, similar to the pre-edge feature from layered $K_2Ti_2O_5$. It is noted that nanosheet/nanotube products with five-coordinate titanium were synthesized during hydrothermal treatments.

As mentioned in Figure 7, in the primary stage of hydrothermal treatment, the nanosheet-like products (layered sodium titanate) were preferentially formed and, subsequently, their nanosheets were exfoliated from layered sodium titanate and then the nanosheets were curled and scrolled to nanotubes. Thus, the nanotubular products composed of sodium titanate were formed by exfoliation and scrolling up of these nanosheet-like products/nanosheets during these hydrothermal treatments. Consequently, from these results, it is obvious that distortion of the octahedral TiO_6 unit increased with progression of the hydrothermal reaction and finally led to formation of the five-coordinate titanium species, judging by the fact that both peaks C and B increased with hydrothermal treatments.

However, the XANES spectrum of nanotube products prepared by hydrothermal treatments for 96 h, in which the hydrothermal reaction from anatase to nanotube products was completely finished, was a little different from layered $K_2Ti_2O_5$ as a reference, especially around peak C. Although peak C is confirmed for the product prepared by hydrothermal treatment for 96 h in the pre-edge spectrum of Ti K-edge XANES, this peak C may be derived from the anatase structure. The nanotubes prepared by hydrothermal treatments for 96 h may contain partly anatase-like structure, because peak C still remains after the hydrothermal reaction for 96 h, as shown in Figure 11. Although there is no denying that nanotube products possess, in part, the anatase-like structure, the detailed study is under investigation.

4. Conclusions

In this study, the structural change on the molecular scale of anatase-type TiO_2 during hydrothermal treatment was investigated in detail by various analytical techniques such as XAFS, TEM, and so on, in order to clarify the formation mechanisms of titanate-based nanotubes prepared by a hydrothermal process. According to TEM observation, it was found that the nanosheet-like products and nanosheets

(44) Anderson, S.; Wadsley, A. D. *Acta Chem. Scand.* **1961**, *15*, 663.
(45) Chen, L. X.; Rajh, T.; Wang, Z. Y.; Thumauer, M. C. *J. Phys. Chem. B* **1997**, *101*, 10688.
(46) Grunes, L. A. *Phys. Rev. B* **1983**, *27*, 2111.
(47) Farges, F.; Brown, G. E.; Rehr, J. J. *Geochim. Cosmochim. Acta* **1996**, *60*, 3023.
(48) Kriventsov, V. V.; Kochubey, D. I.; Tsodikov, M. V.; Navio, J. A. *Nucl. Instrum. Methods Phys. Res.* **2001**, *470*, 331.

were generated on the surface of an anatase-type TiO_2 particle by hydrothermal treatment of anatase-type TiO_2. Ti K-edge XAFS results implied that these nanosheet-like products and nanosheets were composed of highly distorted TiO_6 octahedra. From Ti K-edge XANES pre-edge spectra, it was speculated that the anatase-like structures are partially built up with the formative nanotubes by scrolling up of these sheetlike products.

Consequently, in the primary stage of hydrothermal treatment, the nanosheet-like products (layered sodium titanate) were preferentially formed and, subsequently, their nanosheets were exfoliated from layered sodium titanate and then their nanosheets were curled and scrolled to nanotubes. Thus, the nanotubular products composed of sodium titanate were formed by exfoliation and scrolling up of these nanosheet-like products/nanosheets during these hydrothermal treatments.

Acknowledgment. This work was partly supported by the Circle for the Promotion of Science and Engineering (2008) and Grant-in-aid for Scientific Research from Japan Society for the Promotion of Science (Grant 20047011). XAFS measurements were carried out at BL01B1 in SPring8 (Grants 2004B0166 and 2006A-1286). The authors are grateful for the technical support and discussion from JASRI.